

Part 2: Preparation for Wind Tunnel Model Testing and Verification of Cal Poly's AMELIA 10 Foot Span Hybrid Wing-Body Low Noise CESTOL Aircraft

Kristina Jameson¹, David Marshall², Robert Ehrmann³, and Eric Paciano⁴
California Polytechnic State University, San Luis Obispo, CA, 93407

Robert J. Englar⁵
Georgia Tech Research Institute, Atlanta, GA 30332-0844

and

William C. Horne⁶
NASA Ames Research Center, Mountain View, Ca 94043

A collaboration between California Polytechnic Corporation with Georgia Tech Research Institute (GTRI) and DHC Engineering worked on a NASA NRA to develop predictive capabilities for the design and performance of Cruise Efficient, Short Take-Off and Landing (CESTOL) subsonic aircraft. The focus of this work presented in this paper gives details of a large scale wind tunnel effort to validate predictive capabilities for this NRA for aerodynamic and acoustic performance during takeoff and landing. The model, Advanced Model for Extreme Lift and Improved Aeroacoustics (AMELIA), was designed as a 100 passenger, N+2 generation, regional, cruise efficient short takeoff and land (CESTOL) airliner with hybrid blended wing-body with circulation control. AMELIA is a 1/11 scale with a corresponding 10 ft wing span. The National Full-Scale Aerodynamic Complex (NFAC) 40 ft by 80 ft wind tunnel was chosen to perform the large-scale wind tunnel test in the scheduled to start summer of 2011. The NFAC was chosen because both aerodynamic and acoustic measurements will be obtained simultaneously, the tunnel is large enough that the downwash created by the powered lift will not impinge on the tunnel walls, and the schedule and cost fit into Cal Poly's time frame and budget. Several experimental measurement techniques will be used to obtain the necessary data to validate predictive codes being developed as apart of this effort: stationary microphones will be used to obtain far-field acoustic measurements including a 48 element phased array, the Fringe-Image Skin Friction (FISF) technique will be used to measure the global skin friction on the wing, and the a micro flow measurement device will measure the velocity profiles in the in the boundary and shear layers is still in development and presented in this paper.

¹ Assistant Professor, Aerospace Engineering, San Luis Obispo, Ca 93407, AIAA Member.

² Associate Professor, Aerospace Engineering, San Luis Obispo, Ca 93407, Senior AIAA Member.

³ Graduate Student, Aerospace Engineering, San Luis Obispo, Ca 93407, AIAA Student Member.

⁴ Undergraduate Student, Aerospace Engineering, San Luis Obispo, Ca 93407, AIAA Student Member.

⁵ Principal Research Engineer, Georgia Tech Research Institute, Atlanta, GA 30332, Senior AIAA Member.

⁶ Senior Research Engineer, Mountain View 94043, AIAA Member.

Nomenclature

C_f	=	coefficient of skin friction
q	=	dynamic pressure
n	=	oil index of refraction
t	=	time duration
θ_r	=	refraction angle
λ	=	wavelength of light
μ	=	oil viscosity
τ_w	=	wall shear stress

Subscripts

o	=	oil
∞	=	freestream condition

I. Introduction

The recent advent of NASA's Environmentally Responsible Aviation Project (ERA)¹ shows NASA's dedicated to designing aircraft that will reduce the impact of aviation on the environment, there is a need for research and development of methodologies to minimize fuel burn, emission, and a reduction in community noise produced by regional airlines. ERA is specifically concentrating in the areas of airframe technology, propulsion technology, and vehicle systems integration all in the time frame for the aircraft to be at a Technology Readiness Level (TRL) of 4-6 by the year of 2020 (deemed N+2). The proceeding project looking into similar issues was led by NASA's Subsonic Fixed Wing Project and focused on conducting research to improve prediction methods and technologies that will produce lower noise, lower emissions, and higher performing subsonic aircraft for the Next Generation Air Transportation System.

The work provided in this investigation was an NRA funded by Subsonic Fixed Wing Project with a specific goal of conducting a large scale wind tunnel test along with the development of new and improved predictive codes for the advanced powered-lift concepts. These concepts will be incorporated into the wind tunnel model in conjunction with the verification of these codes an experimental data base will obtained during the wind tunnel test. Powered-lift concepts investigated are Circulation Control (CC) wing in conjunction with over the wing mounted engines to entrain the exhaust to further increase the lift generated by CC technologies alone. The NRA was a four year award; during the first year the objective was to select and refine CESTOL concepts and then to complete a preliminary design of a large scale wind tunnel model for the large scale test. During the second and third years the large scale wind tunnel model design would be completed and manufactured. In the fourth and final year the large scale wind tunnel test would be conducted along with the completion of the predictive codes for the advanced powered-lift concepts incorporated into the wind tunnel model in conjunction with the verification of these codes with the experimental data obtained during the wind tunnel test.

The original configuration was developed by David Hall and refined by Cal Poly which was designed as a 100 passenger, regional, cruise efficient short takeoff and land (CESTOL) airliner with hybrid blended wing-body with circulation control.. The wind tunnel model was sized by the NRA and the size of available wind tunnels, which scaled the model to a 10 ft span. The resulting design is the Advanced Model for Extreme Lift and Improved Aeroacoustics (AMELIA) and is the subject of two companion papers. Part 1 of this paper (The Wind Tunnel Model Design and Fabrication of Cal Poly's AMELIA 10 Foot Span Hybrid Wing-Body Low Noise CESTOL Aircraft) describes the conceptual designs considered for this project, the selected configuration adapted for a wind tunnel model, the internal configuration of AMELIA, and the internal experimental measurements chosen in order to satisfy the requirement of obtaining an experimental measurement database. Part 2 of this paper will describe the progress of the large-scale wind tunnel test along with the external experimental techniques that will be employed during the test. Experimental measurements included in the database will include forces and moments and surface pressure distributions (covered in detail in Part 1), along with local skin friction measurements, boundary and shear layer velocity profiles, far-field acoustic data and noise signatures from turbofan propulsion simulators (which is the subject of this investigation). Currently, the test is scheduled as an 8-10 week test with a tunnel entry date in the late summer of 2011.

II. AMELIA Model

The model is approximately a 1/11 scale of an aircraft designed as a 100 passenger, N+2 generation, regional, cruise efficient short takeoff and landing (CESTOL) airliner with a hybrid blended wing-body and circulation control designed by David Hall and refined by Cal Poly. The N+2 design metrics are: a 40% reduction in fuel consumption, progress towards -42 dB lower noise levels, a 70% decrease in emissions, and a 50% reduction in field length performance over current generation aircrafts. Theoretically the aircraft should reach a Technology Readiness Level (TRL) of 4-6 by the year 2020. A conceptual design of the AMELIA is shown in Fig1 where the complicated internals of AMELIA are shown in Fig. 2. For a full description of the wind tunnel model design and manufacturing progress please refer to: Part 1: The Wind Tunnel Model Design of Cal Poly's AMELIA 10 Foot Span Hybrid Wing-Body Low Noise CESTOL Aircraft.

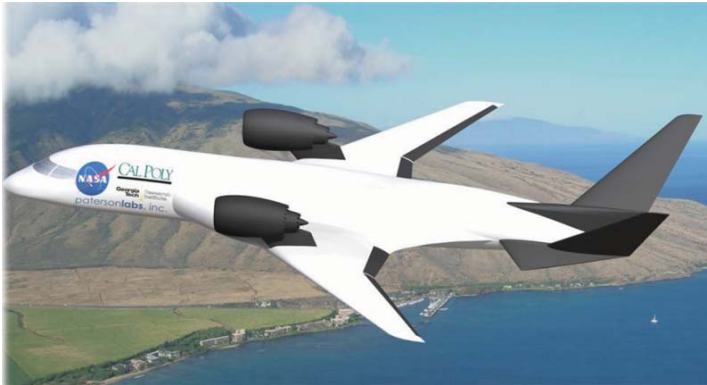


Figure 1. An artists rendition of AMELIA flying over Hawaii.

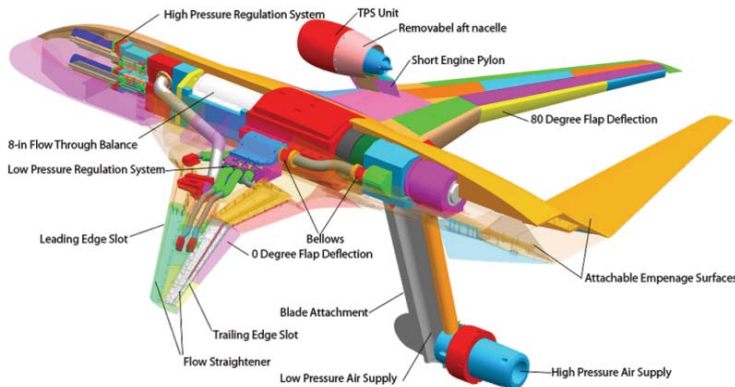


Figure 2. A view of AMELIA revealing the complex internal components.

NFAC wind tunnel with the associated acoustic measurement devices mounted on the tunnel floor relative to the wind tunnel model placed in the center of the tunnel. Also depicted in Fig. 3 is a preliminary CFD result of the flow features expected from the interaction of the upper surface blowing and the circulation control powered lift system. The downwash of the powered lift system is estimated to be approximately a full span down from the model.

III. Large Scale Wind Tunnel Test – NFAC 40 ft by 80 ft’

A. Wind Tunnel Facility

The National Full-Scale Aerodynamic Complex (NFAC) 40 ft by 80 ft wind tunnel was chosen to perform the 8-10 week long large scale wind tunnel test. The NFAC offered several benefits over other large wind tunnels across the country, with the most significant being: the 10 foot model could be mounted on a sting which allows for cleaner measurements of the produced aerodynamic forces and moments, the tunnel could supply the high pressure air at the mass flow rate necessary to operate the CCW slots and the turbofan simulators, the tunnel is large enough such that the downwash created by the CCW wings would not impinge on the floor of the tunnel thus creating cleaner far-field acoustic measurements, the tunnel was acoustically treated such that aerodynamic and acoustic measurements could be performed simultaneously, and the NFAC’s cost and schedule fit within Cal Poly’s time frame and budget. Figure 3 shows a scale schematic of the model mounted on the sting in the 40 ft by 80 ft

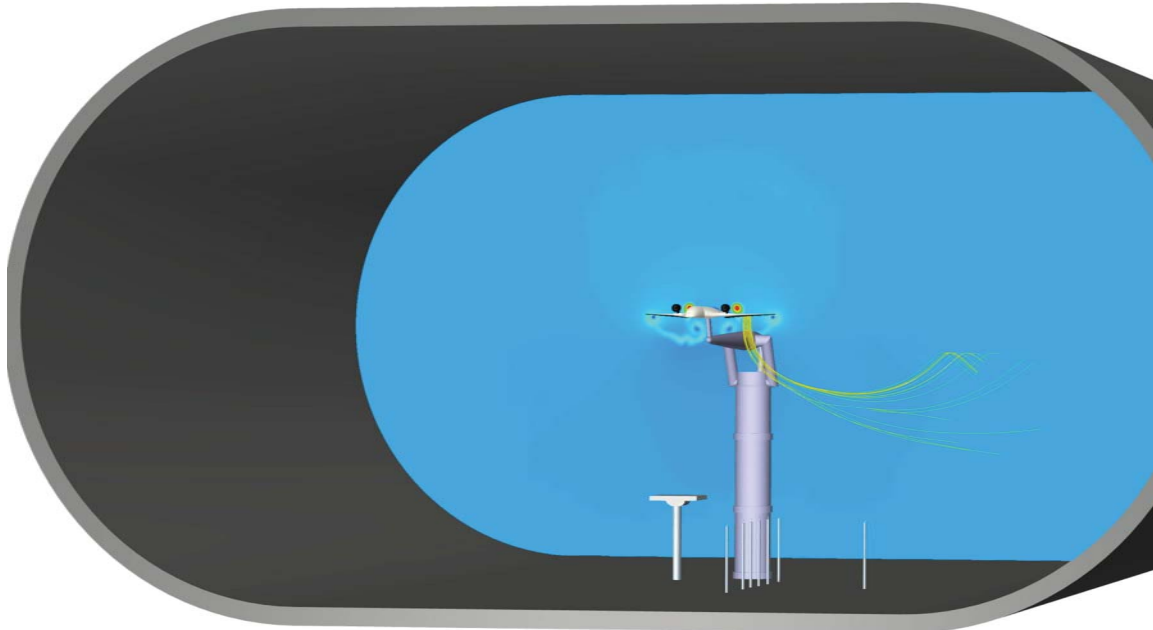


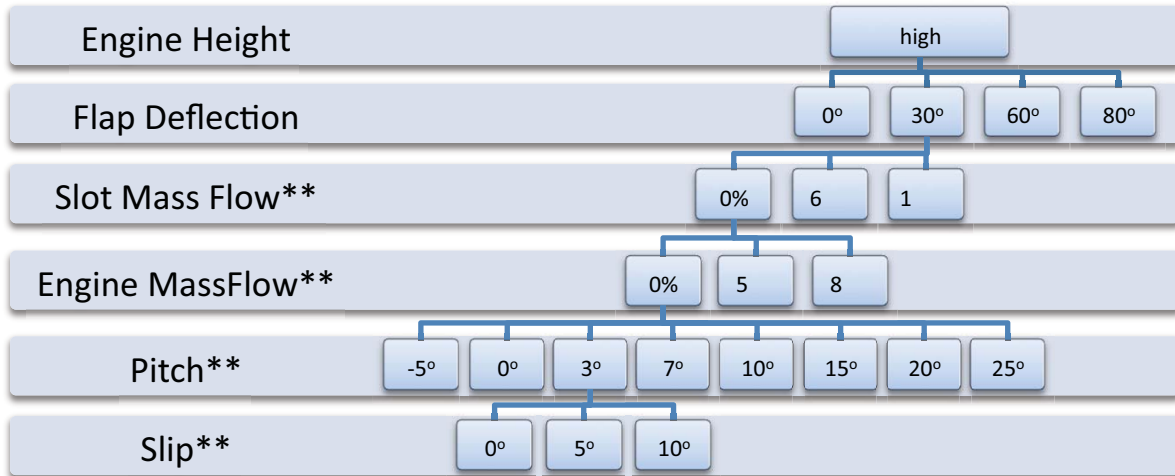
Figure 3. Schematic of the model mounted on sting in the NFAC 40 ft by 80 ft wind tunnel along with the far-field microphones and the stationary array mounted on the tunnel floor.

B. AMELIA Test Matrix

The tunnel time for the AMELIA test will be 8-10 weeks depending on the schedule and cost provided to Cal Poly by the NRA. The proposed outline of the test matrix for AMELIA the Steps are as follows: (1) calibrations while mounted on the sting balance of both model and acoustic instrumentation, (2) static tests of all blown features on the model, (3) a Reynolds number sweep, (4) a dynamic pressure sweep, (5) a turbofan simulator sweep, (6) and a CCW sweep, (7) acquire critical test points, and (8) acquire experimental data base measurements. After the completion of the preliminary sweeps [Steps 1-6], during Step 7 eight to ten critical tests points will be identified from the experimental test data obtained during the preliminary sweeps. The purpose of Step 7 is to take the full gamut of experimental measurements. The skin friction measurements (see Section V. Global Skin Friction Measurements for further detail) are the dominating measurements and will take upwards to two hours per critical test point to obtain functional data. Due to budget and schedule, only 8-10 critical test points will be acquired. The wind tunnel test will be considered successful if Steps 1-7 are completed. During the critical tests points all experimental instrumentation will be utilized: such as the four different flap configurations (0° , 30° , 60° , and 90°), the high and low engine mounting, slow flow, and engine mass flow.

Once the critical test points have been completed, the remaining time will be used during Step 8 to obtain the experimental data base, however the skin friction technique will not be utilized during this portion of the test. Table 1 outlines the proposed Step 8 test matrix starting with the most time consuming model modification. The ranges for pitch are $+20$ to -5 degrees, side slip can vary from $+20$ to -20 degrees, three different momentum coefficients will be investigated (0, 66%, and 100 of the maximum), three different thrust coefficient will be investigated (engine thrust levels of 0, 48, and 80% of the maximum rate level), and for three different tunnel speeds. During Steps 1-8 the acoustic the far-field measurements along with 30 degree sideline measurements will simultaneously be made with the aerodynamic measurements. Also the 48 element stationary array placed under one of the turbofan simulators will be utilized to characterize the noise signature beneath the wing.

Table 1. Outline of the experimental data base test matrix to be completed once the 8-10 critical test points have been obtained.



IV. Aeroacoustic Measurements

Acoustic measurements for the large wind tunnel test will consist of seven microphones 16 ft under the left wing near the fly-over arc at 45, 60, 75, 90, 105, 120, and 135 deg. from the upstream direction, as well as a 48-element, 40 inch diameter (1 meter) phased microphone array housed in a streamlined fairing under the right wing near the 90 deg fly-over angle. Three additional microphone pairs will be positioned on the right side near the peak jet noise location with direct view of the TPS units to help estimate shielding effects. These three struts will have a dual microphone system for redundancy due, it would time and cost prohibitive to replace this set of microphones if a failure should occur. Figure 4 shows a schematic of the acoustic measurement devices mounted in the NFAC with AMELIA mounted on the sting. While Fig. 5 is 3D schematic of the NFAC tunnel floor with the associated acoustic measurement devices. During a test condition where sideslip will be investigated, notice in that the far-field and phased array will rotate with the model while the sideline microphone struts will remain stationary.

The array and fixed microphones will use TMS-140BF(G.R.A.S. 40 BF) 1/4" condenser microphones, with TMS126 AC (G.R.A.S. 26AC) pre-amplifiers and G.R.A.S 12AG power supplies. The processing bandwidth will be 1 to 40 kHz model scale (0.1 to 4 kHz full-scale) Array signal processing and display will utilize Optinav Beamform Interactive software. Evaluation and integration of the commercially available software at speeds planned for the AMELIA test for have been accomplished during preliminary test programs in the NFAC 80- by 120- Ft Wind Tunnel, as well as in the NASA AOX 32- by 48 inch Wind Tunnel at the Ames Fluid Mechanics Laboratory.

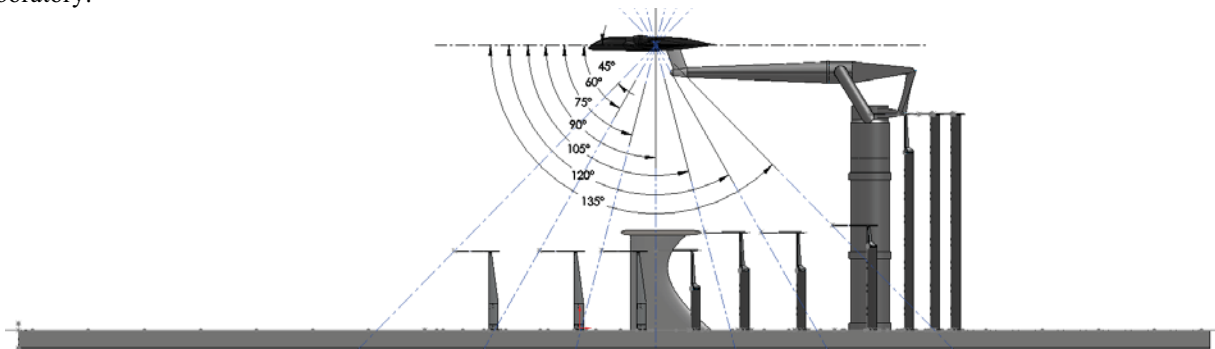


Figure 4. A schematic of AMELIA mounted in the NFAC showing the far field, sideline, and phased array microphones in scale reference to the model.

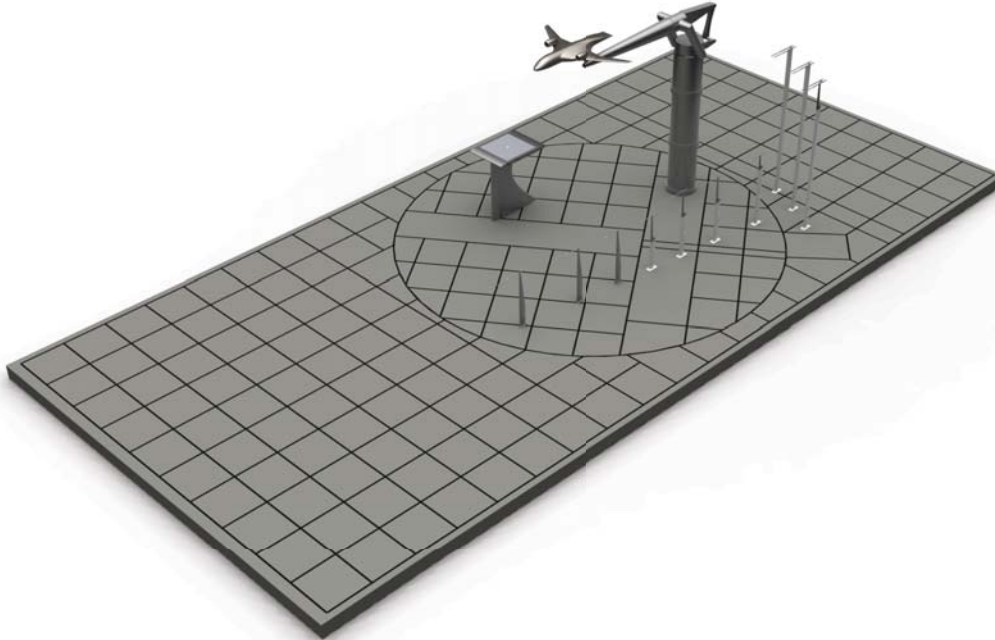


Figure 5. A 3D rendering of the aeroacoustic measurements and AMELIA mounted in the NFAC; note that the stationary far field microphones and phased array have the ability to rotate with the model during sideslip investigations but the 30 degree sideline microphones will remain stationary.

V. Global Skin Friction Measurements

The Fringe-Image Skin Friction (FISF) Technique, also known as oil interferometry, was chosen for the large scale wind tunnel test to measure skin friction because both magnitude and direction can be determined from a single image. The FISF technique has the advantage of maturity and reliability which becomes significant due to the difficulties of obtaining measurements in the NFAC due to its sheer size and the amount of time between tunnel shut down and the point where photographs of the model can be obtained.

A. FISF Technique

The FISF technique was developed by Monson et al.² The theory behind the technique is that a single relationship can relate the thickness of the oil drop at a single location to the skin friction magnitude and direction. The oil thickness is measured via photographic interferometry. Data reduction is completed with CXWIN4GG, a PC application developed by Zilliac.³

The FISF technique has a few key steps in its process to obtain the crucial photographs necessary to determine surface skin friction. The process is as follows: A drop of silicone oil of known viscosity is placed on the model surface. Once the oil is applied to the surface, the air flow begins, causing the oil to spread and thin. The air continues to flow for a given time, continually thinning the oil. When sufficient time has elapsed (2-20 minutes, depending on oil viscosity), the air flow is turned off. A quasi-monochromatic light source is then indirectly applied to the surface by use of a large diffuse reflector. Light is reflected from the surface of the model and oil. Two specific light rays are reflected and separated by the thickness of the oil, shown in Fig. 6. Once the oil has thinned, the oil height linearly varies where constructive and destructive interference occurs, causing light and dark fringes on the oil surface. Skin friction is proportional to the spacing distance, Δs , on the fringes which is directly related to the thickness of the oil. The relationship for skin friction is as follows:

$$C_f = \frac{\tau_w}{q_\infty} = \frac{2n_o \mu_o \Delta s}{q_\infty \lambda t} \quad (1)$$

where C_f is the skin friction coefficient, τ_w is the wall shear stress, q_∞ is the freestream dynamic pressure, n_o is the oil index of refraction, μ_o is the oil viscosity, λ is the wavelength of the light source, t is the duration of time the oil flow was exposed to air flow, and θ_r is the light refraction angle through the air-oil interface. Eq. 1 holds for zero pressure gradient and shear stress gradients. Further details on the oil flow technique and theory behind it is covered by Naughton and Sheplak.⁴

B. Application of FISF to AMELIA

In order to successfully apply the FISF technique, the fringes on a model need to be clearly visible. Fringe visibility is based upon the surface finish of the model. An ideal surface is extremely smooth with consistent and durable optical properties. Based on a study by Zilliac⁵ the best fringes appeared on high flint content SF11 glass manufactured by Schott Glass of Germany, which is an impractical material for a wind tunnel model. A practical surface finish for a model would be mirror like, which can be achieved with nickel plating the model surface. Acceptable substitutes have been made utilizing polished stainless steel or black Mylar sheets applied to the model surface. Black Mylar sheets offer the most cost effective solution for oil flow testing. However, at higher speeds and long run times Mylar would begin to peel along the edges, ruining any data downstream. The continual Mylar reapplication to the model would prove time consuming and impractical due the model height in the NFAC for the AMELIA test. Mylar is also difficult to apply to a 3D surface, usually resulting in small wrinkles in the Mylar distorting the skin friction measurements. Polished stainless steel and nickel plating have the durability that Mylar lacks. Nickel plated aluminum is less expensive than polished stainless steel. For these reasons, a nickel plated aluminum was initially chosen for the large scale wind tunnel test. Unfortunately, the due to the size of the model, nickel plating became nearly impossible and cost prohibitive and therefore another alternative had to be found. It was decided that IMRON paint would be an adequate replacement due to its highly reflective surface finish.

In order to properly view the fringes, a monochromatic light source must be reflected off a diffuse reflector. In large wind tunnel applications, the tunnel walls have been used as the rector.⁶ Unfortunately, the NFAC tunnels walls are composed of a matte metal mesh covering a deep, perforated acoustic liner, rendering the walls unable to sufficiently light the tunnel. The next option is to build a reflector which encompasses the portion of interest on the model. A small hole would be cut in the reflector allowing a camera to capture the fringe spacings; a setup such as this is shown in Fig. 4. AMELIA has a highly curved blended wing which causes additional difficulty in the image processing. Due to the models highly polished and curved surfaces, the camera will see reflections from a large area of the wind tunnel. Therefore, if the wind tunnel is being used as the diffuse reflector, large areas of the tunnel need to be white. Since this would be costly in the NFAC, it is necessary to use a curved diffuse reflector. It will ensure the model is uniformly lit allowing for accurate fringe spacing identification and does so with fewer lights. The type of diffuse reflector used on the wing blend is also shown in Fig. 7.

The angle at which the light enters the camera can greatly affect the skin friction measurement, especially at large angles such as leading edges or the blended wing portion of the model. Zilliacs CXWIN4GG software utilizes single camera photogrammetry to determine the angle of the light reflecting off the oil on the surface of the wind

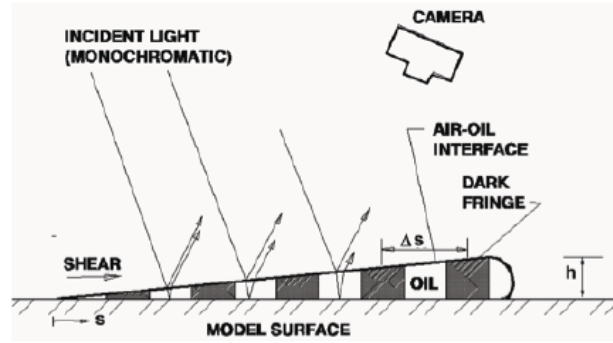


Figure 6. A schematic of the basic FISF setup highlighting the oil flow and fringe pattern on a droplet of oil from Reference 4.

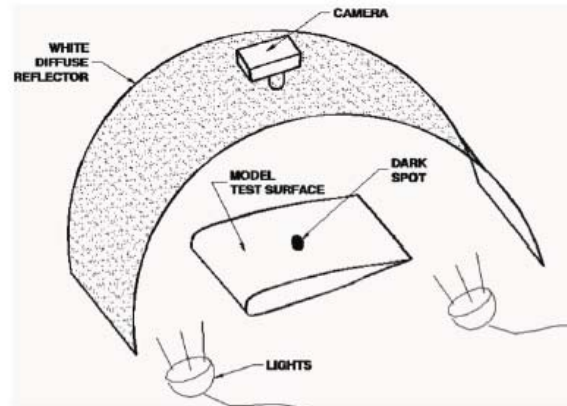


Figure 7. The FISF solution used for the wing blend. The dark spot is due to no light being reflected by the camera lens.

tunnel model. This is made possible by using fiducial marks over the model surface. The camera captures an image encompassing the entire wing with several fringes over the wing surface. Within that image are multiple fiducial marks with known locations on the model coordinate system. Ziliacs software completes the photogrammetry by matching the known fiducial marks locations (both a pixel x-y coordinate system as well as the model coordinate) to a given set of model points. This allows the software to calculate the light incident angle at any visible point on the model.

Due of the size of the NFAC, a special procedure has been devised to ensure accurate fringe production. Normally the tunnel transients are short, resulting in little error from the startup and shutdowns. However, the NFAC requires a minimum of 5 minutes to startup and shutdown which can introduce unacceptable error into the skin friction measurements if the incorrect viscosity of oil is chosen for the test. In order to ensure recording accurate fringes, the model will be at a high angle of attack during the tunnel startup allowing separated flow (low to no shear) over the wing. Once the tunnel freestream has been reached, the model will be positioned to the angle of attack of interest. At this point, slot blowing and the turbine simulators will be started as well. The model will remain at this test condition for a minimum of 20 minutes. Once the oil is sufficiently spread, the slot blowing, turbine simulator, and tunnel freestream will be turned off, while the model is once again pitched upward to cause separation over the wing allowing the fringes to be unaffected by the shutdown procedure. Once the flow has stopped, the diffuse reflector and camera will be brought into the tunnel. A diffuse reflector will be held up to the model, lighting it, while a second person will capture the fringe spacings in two images. This process is time consuming, but worthwhile to ensure quality data for numerical validations to be made against. For this reason, again only eight to ten key test conditions will be investigated with oil interferometry for CFD validation.

B. Application of FISF to a Blended Wing Section

In order to prepare for the skin friction measurements on AMELIA first skin friction magnitude and direction measurements will be completed on the three-view of wing section shown in Fig. 8. The blended portion (the shaded portion of the three-view shown in Fig. 8 is representative of the wing blend on AMELIA. The lighting technique and wind tunnel procedure are similar to the AMELIA test, aiding in the preparation for the AMELIA test. In addition, the test will create a database of global skin friction measurements for CFD validation on a blended wing geometry. The two foot wing section was manufactured by Patersonlabs, Inc. Ideally, a scale model of the AMELIA wing blend would have been made, but a size constraint was placed on the test article by the demotions of the wind tunnel available for the pretests at Cal Poly and by the stock available at Patersonlabs, Inc. to reduce cost of the article. The test article chord needed to be less than 6 inches, have a thickness of less than 3 inches, and must have the ability to remove the model from a 6 inch wind tunnel access hole. For this reason, a long 2D section was machined, with a small 3D section at the outboard. Note that the lower surface of the test article does not match AMELIA. To correctly blend the upper and lower surfaces, the 2D chord length would have to be scaled down to a point too thin to reasonably manufacture. It was most important to match the upper surface of the test article to AMELIA, so the blended airfoil was shifted up, causing the lower surface to not match AMELIA.

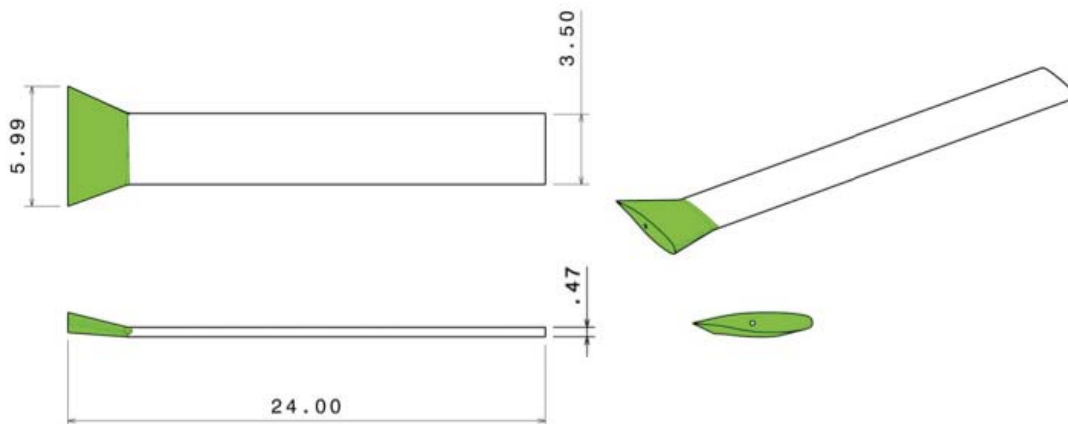


Figure 8. Three view of blended wing where the 3D wing blend section is shown in green and the 2D section is left white (all dimensions are in inches).

The test article for the pretest experiment was also nickel plated to allow as many similarities to the AMELIA test as possible. Additional 2D experiments were conducted Imron painted aluminum to ensure fringe quality. The plating and Imron paint has yielded excellent fringe visibility; a comparison is shown in Fig. 9. The fringes shown were created using high pressure air and a half cylinder white diffuse reflector. The full wing was tested in the Cal Poly Mechanical Engineering 2x2 foot low speed tunnel. Multiple test conditions were investigated to ensure repeatability in NFAC. For the full results please refer to Ref. 10. This practice test was conducted with a similar tunnel start/shutdown procedure that is currently planned for AMELIA.

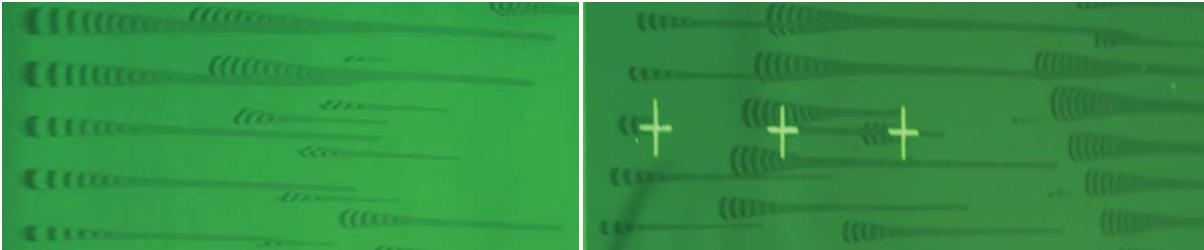


Figure 9. Fringe on test (a) nickel plated sample and (b) an Imron painted sample; The exposure time was increased for the Imron sample, but the comparison between (a) and (b) show good quality fringes for both samples, both samples using 10cSt oil and compressed air to create fringe lit with a diffuse reflector and mercury vapor bulbs.

VI. Boundary And Shear Layer Velocity Profiles with a Micro Flow Measurement Device

A. Cross Correlation Measurement Technique

In 2001, NASA Glenn developed a thermocouple boundary layer rake which has the capability to measure 0.0025 inches from the surface, four times closer than any state of the art measurement before. **Error! Bookmark not defined.**⁴ This was achieved with the device shown in Fig. 10. This device is constructed with a base made out of aluminum, a constant thickness strut which protrudes from the base, and the necessary electrical wires corresponding to the number of thermocouples present for a given design. The strut is made of quartz, chosen for its insulative and low thermal expansion properties. From the base to the top of the strut, there are several pairs of thermocouples. The device functions based on the theory that for a given height above the base, the velocity is equal to the velocity of the flow as if there were no strut present. It should be noted that no horseshoe vortices were found to be shed at the intersection of the strut and base in NASA Glenn’s testing of the thermocouple rake.⁷

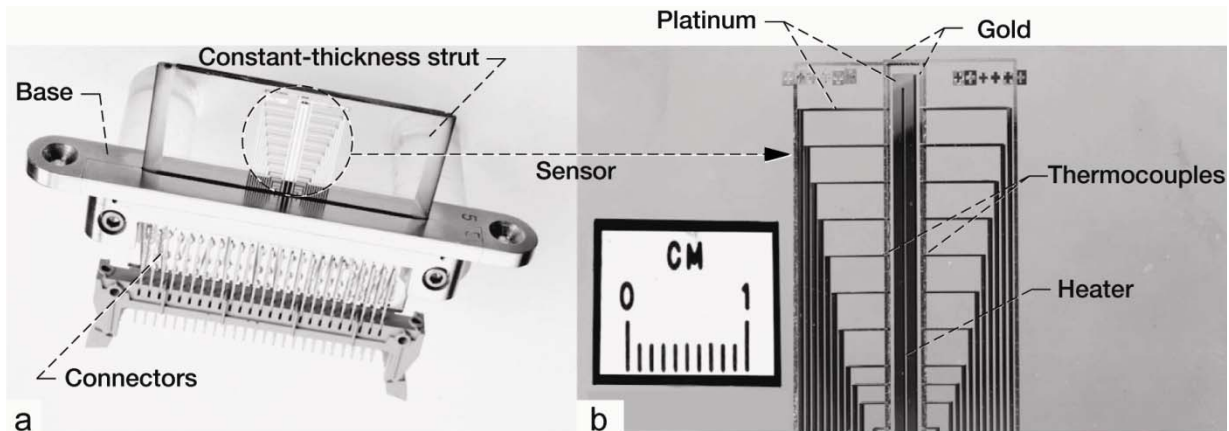


Figure 10. Photographs of a thermocouple boundary layer rake, a) shows the base and electrical connections and b) detail of platinum and gold films.¹⁵

At the center of the strut, there is a platinum loop which is heated to a temperature above ambient. As air flows over the loop, the air downstream is heated. The voltage difference between the upstream and downstream thermocouples is then related to known velocity values obtained from a total pressure rake setup next to the thermocouple rake at exactly the same axial position. A calibration curve can be developed from this data. This calibration procedure is needed for every Reynolds number intending to be tested.

Upon further discussions with Gustave Fralick, one of the thermocouple rake's designers, a Cross Correlation Rake (CCR) was suggested for use since an in situ calibration process would prove difficult in the anticipated application. The CCR contains a conductive platinum loop located at the center of the substrate. This loop is heated to a temperature above the ambient conditions. Instantaneous voltage differences on the loop's leading edge and trailing edge are measured by voltage taps along the loop. The voltage fluctuations in the loop are caused by fluctuations in the local resistance. The resistance relates to the loop temperature, which relates directly with velocity at that location.⁸ Utilizing a cross correlation script from MATLAB, the time between voltage fluctuations on the upstream and downstream voltage taps can be calculated. Since the distance between the upstream and downstream edges of the loop is known, the flow velocity can be calculated.

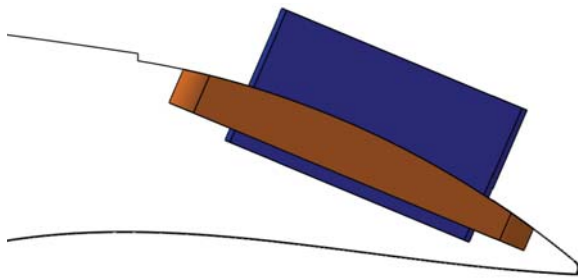


Figure 11. A rendering of the Cross Correlation Rake applied to the AMELIA flap where the airfoil section is shown as an outline. The CCR is shown with an orange base and blue quartz substrate.

B. Application of CCR to AMELIA

The AMELIA model has both leading and trailing edge blowing in order to vastly increase the lift. Part of the validation effort will be to acquire velocity profiles above the flap. The CCR will be implemented as shown in Fig. 11 in order to achieve this. This region is of particular interest because of the jet's layer boundary layer as well as the shear layer above the jet. The design, construction, and validation of the CCR at subsonic speeds will be achieved. In addition, transonic speeds should be tested to demonstrate the CCR readiness on AMELIA. The substrate was constructed at Cal Poly, with the platinum applied to the substrate at NASA Glenn. The CCR will first be

applied to a flat plate for validation purposes, then a trailing edge of an airfoil.

The CCR designed for the AMELIA test is composed of a quartz substrate, platinum heating loop, and platinum voltage taps, as shown in the schematic in Fig. 12 and in the photograph in Fig. 13. The CCR was sized based on the AMELIA flap and was sized to 1.1 x 0.55 inches and 0.043 inches thick. It needed to be as large as possible without being too near to the slot or trailing edge. The resulting length was 1.00 inch. The height was based upon the desired height above the flap to measure velocity profiles. This height was determined to be 0.12 inches. The total height of the rake is 0.040 inches, with the top half above the flap and the remaining lower half below the flap. Quartz microscope slides from Ted Pella, Inc. were utilized as the substrate. Microscope slides were only sold at a thickness of 1.0 mm. For a full description of the CCR design process please refer to Ref. 13.

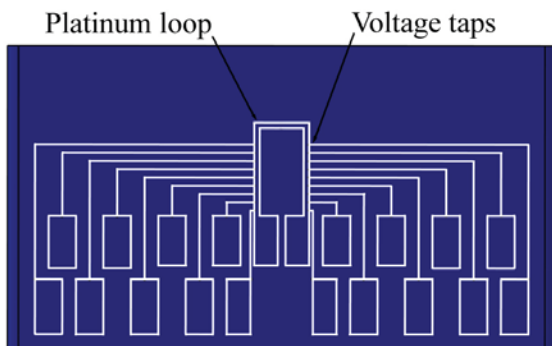


Figure 12. Schematic of the Cross Correlation Rake with platinum loop and voltage taps shown.

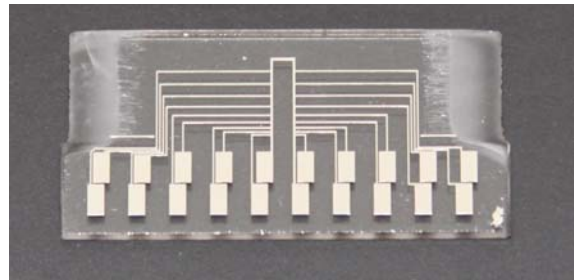


Figure 13. Photograph of the Cross Correlation Rake of the first batch of rakes delivered to Cal Poly.

C. Validation of CCR

Application of the CCR to the AMELIA test will yield valuable data for CFD validation. Velocity measurements of both the jet boundary layer and jet shear layer will be acquired. The CCR span location was chosen to be far from the engine, wingtip, or chord variation effects. An outboard location of 36.6 inches from the centerline was chosen, shown in Figure 14a. The rake was placed perpendicular to the trailing edge slot to ensure the substrate incurs no flow angularity. The rake is also perpendicular to the flap dihedral. As the flap deflects, the rake position is held constant relative to the flap trailing edge.

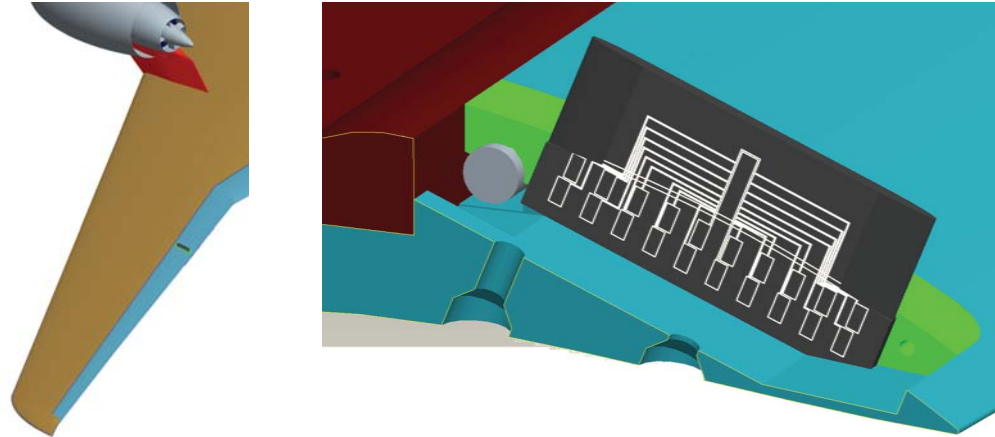


Figure 14. Isometric view (a) of the CCR applied to a rendering of the AMELIA wing and (b) substrate (dark grey), half of CCR base (green), flap (blue) and bottom of wing plenum (red). The platinum mask is shown overlaid on the rake. The light grey circular tube carries the CCR wiring inboard. Two white curved lines represent the flap upper surface relative to the platinum mask.

Application of the CCR to the AMELIA test will yield valuable data for CFD validation. Velocity measurements of both the jet boundary layer and jet shear layer will be able to be acquired. The CCR span location was chosen to be far from the engine, wingtip, or chord variation effects. An outboard location of 36.6 inches from the centerline was chosen, shown in Figure 14b. The rake was placed perpendicular to the trailing edge slot to ensure the substrate incurs no flow angularity. The rake is also perpendicular to the flap dihedral. As the flap deflects, the rake position is held constant relative to the flap trailing edge. AMELIA was designed with four flap settings, each having an offblock allowing for CCR installation. There is one universal base for the CCR which fits into the offblock locations in each flap. The Omnetics micro connector allows for simple and rapid removal of the CCR wiring.

At the time of this paper publication, it has been decided that the CCR's technology is not mature enough for the large scale wind tunnel test in the summer of 2011. However, the CCR does provide a unique capability of measuring the velocity and shear layer profiles, and merits further research. Cal Poly will continue its work on the CCR in pursuit of the CCR reaching a high enough fidelity that it will be a viable option in large scale wind tunnel testing in the future.

Acknowledgments

The authors would like to acknowledge the NASA Research Announcement award under Contract i#NNL07AA55C, with technical monitors Craig Hange and Clif Horne, who provided funding for this work. The authors wish to thank the Ames Research Center's Fluid Mechanics Lab, in particular, Gregory Zilliac and David Driver for the assistance in applying the technique to AMELIA. The authors would also like to thank NASA Glenn, especially Gustave Fralick for his time and assistance. Lastly, a special thanks to Russell Westphal for his sharing of expertise and supplies.

References

- ¹Marshall, D., Jameson, K., Golden, R., Welborn, A., Erhmann, R., "NRA Final Year One Report," NASA NRA, 2008.

- ²Monson, D. J., Mateer, G. G., and Menter, F. R., "Boundary-Layer Transition and Global Skin Friction Measurements," SAE 932550, Society of Automotive Engineers, Costa Mesa, CA, September 1993.
- ³Zilliac, G. G., "The Fringe-Imaging Skin Friction Technique PC Application User's Manual," NASA Technical Memorandum 1999-208794, NASA Ames Research Center, Moffett Field, CA, September 1999.
- ⁴Naughton, J. W. and Sheplak, M., "Modern Developments in Shear-Stress Measurement," *Progress in Aerospace Sciences*, Vol. 38, No. 1, 2002, pp. 515-570.
- ⁵Zilliac, G. G., "Further Developments of the Fringe-Imaging Skin Friction Technique," NASA Technical Memorandum 110425, NASA Ames Research Center, Moffett Field, CA, December 1996.
- ⁶Driver, D. M. and Drake, A., "Skin-Friction Measurements Using Oil-Film Interferometry in NASA's 11-Foot Transonic WindTunnel," *AIAA Journal*, Vol. 46, No. 10, October 2008, pp. 2401-2407.
- ⁷Hwang, D., Fralick, G. C., Martin, L. C., Wrbanek, J. D., Blaha, C. A., "An Innovative Flow Measuring Device- Thermocouple Boundary Layer Rake," NASA/TM—2001-211161, December 2001.
- ⁸Fralick, G., Wrbanek, J. D., Hwang, D., and Turso, J., "Sensors for Using Times of Flight to Measure Flow Velocities," *NASA Technical Briefs*, LEW-17944-1, July 2006.
- ⁹The Mathworks Inc., Natick, MA, MATLAB, 7th ed., 2008.
- ¹⁰Ehrmann R, Paciano E, and Jameson K K. "Application of the FISF technique to a blended, 2-foot wing section." *28th AIAA Applied Aerodynamics Conference*, Chicago II, AIAA-2010-4830, 2010.
- ¹¹Fralick G, Wrbanek J D, Hwang D, and Turso J. "Sensors for using times of flight to measure flow velocities." *NASA Technical Briefs*, LEW-17944-1, 2006.
- ¹²The Mathworks Inc., Natick, MA, MATLAB, 7th ed., 2008.
- ¹³Ehrmann R, and Jameson K K. "Design and fabrication of a micro flow measurement device." *40th Fluid Dynamics Conference and Exhibit*, Chicago II, AIAA-2010-4622, 2010.
- ¹⁴Hwang, D., Fralick, G. C., Martin, L. C., Wrbanek, J. D., and Blaha, C. A., "An Innovative Flow Measuring Device: Thermocouple Boundary Layer Rake," NASA/TM—2001-211161, December 2001.
- ¹⁵Fralick, G., Wrbanek, J. D., Hwang, D., and Turso, J., "Sensors for Using Times of Flight to Measure Flow Velocities," *NASA Technical Briefs*, LEW-17944-1, July 2006.
-